铝脉冲 MIG 焊亚射流过渡自适应控制熔滴过渡行为分析

杨立军[1]， 李志勇[2]， 李 桓[1]， 李俊岳[1]
（1. 天津大学 天津市现代连接技术重点实验室，天津 300072；2. 中北大学 材料学院，太原 030051）

摘 要：在铝脉冲 MIG 焊亚射流过渡的自适应控制条件下，研究了亚射流过渡的熔滴过渡行为. 对不同脉冲 MIG 焊参数条件下产生的短路过渡、亚射流过渡以及射滴过渡行为进行了电参数波形检测和高速摄像，研究了亚射流过渡发生的条件，分析了在熔滴过渡过程中主要作用力的影响以及表面张力在熔滴形成和过渡过程中的重要作用，指出自适应控制进程中应注意控制的精确化以适应铝 MIG 焊亚射流过渡较窄的工作区间. 结果表明，精确控制焊接参数可以使电弧运行于亚射流过渡的范围并保持亚射流过渡过程的稳定.

关键词：铝；脉冲熔化极氩弧焊；自适应控制；熔滴过渡；高速摄像
中图分类号：TG433 文献标识码：A 文章编号：0253－360X(2009)08－0017－04

杨立军

0 序 言

铝 MIG 焊是一种重要的铝焊接工艺，其熔滴过渡方式有滴状过渡、射滴过渡、短路过渡和亚射滴过渡等几种，各有其过程不同的物理特征. 滴状过渡是在电流较小时的熔滴过渡方式；当电流超过射滴过渡临界电流后，熔滴过渡方式变为射滴过渡. 亚射滴过渡习惯上称为亚射流过渡，是介于射滴过渡和短路过渡之间的一种熔滴过渡方式，弧长较短. 在电弧热的作用下，熔滴形成长大，在形成缩颈即将以射滴方式脱离焊丝之际与熔池短路，完成过渡.

亚射流过渡的熔滴短路时间极短，电流上升不大，缩颈就断裂. 铝 MIG 焊亚射流过渡有非常强的电弧固有自调节作用，其过渡的区间很窄，弧长短，不易控制[1]. 而且对弧长的控制主要是通过检测弧压来进行的，而亚射流过渡区弧长变化引起的弧压变化较小，变化区间很窄，并且电流越小，这种弧压变化的区间越窄. 因此，文中提出了一种铝脉冲 MIG 焊亚射流过渡的自适应控制方法，进行亚射流过渡过程的控制，并在此基础上研究铝脉冲 MIG 焊熔滴过渡的物理特征.

1 控制策略

图 1 示出了一种铝 MIG 焊的熔滴过渡方式的分布[1,2]. 铝及铝合金 MIG 焊一般采用射滴过渡和亚射流过渡.

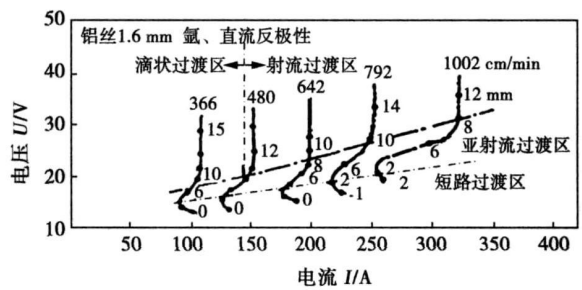

图 1 铝 MIG 焊熔滴过渡形式分布

Fig. 1 Metal transfer distribution in Al MIG welding

产生亚射流过渡的电流、电压值特点是电流一般要超过射滴过渡临界电流，电压又不能太高，而其过渡区间很窄，不易控制.

为克服上述缺点，采用如图 2 所示的脉冲电流自适应控制模式[3]. 图 2 中虚线代表铝 MIG 焊的等熔化曲线（熔化特性曲线），相应的 *ab* 线和 *ed* 线之间的区域在亚射流过渡区内；*mn* 线代表铝 MIG 焊电弧静特性，处于 U 形曲线的上升段；*ae* 线和 *cd* 线代表两条电源恒流特性曲线，*ae* 线电流很小，这样的电流很难形成熔滴过渡，*cd* 线电流较大，位于射流过渡区，足以产生射滴过渡；*bc* 线斜率应大于亚射流过渡区等熔化曲线的斜率.

图 2 所示的控制过程如下：首先假设电弧在 *ae*

收稿日期：2009－01－22
基金项目：国家自然科学基金资助项目（59975068）；天津市自然科学基金资助项目（07JCYBJC04400）

线上燃烧，电压逐渐减小，当电弧电压小于或等于 *a* 点电压时，电流跳至 *b* 点沿 *bc* 线增加，到 *cd* 线电弧电流稳定燃烧；电弧在 *cd* 线上稳定燃烧，电压逐渐增加，当电弧电压大于或等于 *cd* 线上某一点的电压值时，电流跳至 *ae* 线燃烧，进入下一个循环．图 2 中 *a*，*d* 两点的位置选择是关键，*a* 点电压值是电压下限，*d* 点电压值是电压上限．当电弧电压低于 *a* 点电压时，熔滴很容易与熔池短路，进入短路过渡区；当电弧电压高于 *d* 点电压时，很容易进入射流过渡区．*ab* 线斜率，*ed* 线斜率的选择要保证电弧的电流、电压变化处在亚射流过渡区内[3]．

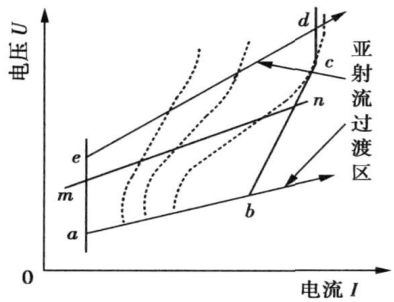

图 2 亚射流电弧的控制

Fig. 2 Arc control of meso-spray transfer

电弧电流越小，亚射流过渡区越窄，*a* 点电压控制及控制点的选取极为重要，此电压值小则易产生短路过渡，大则易产生滴状过渡，影响焊接效果；电弧电流较大时，亚射流过渡区较宽，*d* 点电压选择范围较宽．

2 焊接工艺试验

根据上述铝脉冲 MIG 焊亚射流过渡自适应控制思路，进行工艺试验，选择的几种典型熔滴过渡状态的焊接试验工艺参数如表 1 所示，表中 I_{ae} 代表图 2 中 *ae* 线电流，I_{cd} 代表图 2 中 *cd* 线电流，U_a 代表图 2 中 *a* 点电压，U_d 代表图 2 中 *d* 点电压．其它试验条件为：Ar 保护气流量 15 L/min，焊丝伸出长度 16～20 mm，焊丝 $AlMg_2$/ φ1.6 mm．

铝 MIG 焊产生射滴过渡的临界电流可达 180 A 以上，而焊接电流在 50 A 以下时，则不易产生熔滴过渡．因此，选择脉冲电流为 235 A，远超过射滴过渡的临界电流，基值电流选择为 30 A．

图 3 是铝脉冲 MIG 焊亚射流过渡自适应控制条件下的试验波形，图 3a，c，e 是时基瞬时波形，图 3b，d，f 是其对应的相平面图，表 1 中有各个波形对应的焊接工艺参数．

表 1 脉冲 MIG 焊自适应控制试验参数

Table 1 Experimental parameters of self-adapting control in pulse MIG welding

图号	送丝速度 v_f/(m·min^{-1})	脉冲电流 I_{cd}/A	基值电流 I_{ae}/A	电压上限设定 U_d/V	电压下限设定 U_a/V	电流平均值 I/A	电压平均值 U/V
图 3a，b	3.8	235	30	21.6	14.5	143	18.4
图 3c，d	3.0	235	30	18.8	14.8	122	14.7
图 3e，f	3.8	235	30	23.6	14.5	142	20.7

上述控制过程是一种自适应控制过程，其关键是根据电弧电压值来确定电弧电流的大小，利用脉冲频率的自适应变化，自动将电弧的电流、电压控制在亚射流过渡区内．

从图 3a，b 可以看出，在焊接过程中存在明显的短路过程，但短路时间极短，短路时一般不发生电流的明显上升；其相平面图轨迹密集的核心区域处于较低的电压范围内，却又不是在短路区内，具有明显的亚射流过渡的特征，说明在所采用的控制条件下，焊接过程处于亚射流过渡区．在图 3a，b 焊接工艺参数基础上，降低电压上限的设定值，压低焊接电弧弧长，得到短路过渡发生的情况，如图 3c，d 所示．从图中可以看出，有明显的短路过程存在，且短路时间较长，短路时发生明显的电流上升；其相平面图中的短路区有密集的轨迹分布，类似 CO_2 短路过渡焊的情况，具有短路过渡的特征，说明在降低控制电压后，焊接过程处于短路过渡区．

在图 3a，b 焊接工艺参数基础上，提高电压上限的设定值，提高焊接电弧弧长，得到射滴过渡发生的情况，如图 3e，f 所示．从图中可以看出，无短路过程存在，脉冲电流时间较长，已具有射滴过渡的特征，相平面图中脉冲电流电压的轨迹开始运行于射滴过渡区．

利用脉冲 MIG 焊的亚射流电弧自适应控制，可以将电弧的电流、电压参数控制在亚射流过渡区，但是要实现亚射流过渡，必须选择合适的焊接工艺参数．若参数不合适时，会出现射滴过渡、短路过渡，甚至滴状过渡，从而影响焊接过程和焊接质量．

亚射流过渡、射滴过渡和短路过渡三种熔滴过渡方式各有不同的特点，所进行的同步高速摄像研究如图 4 所示．

图 4a，b 是对应于图 3a 的两组亚射流过渡的高速摄像，从摄像可以看出，亚射流过渡的熔滴在短路的瞬间(图 4a)甚至短路前(图 4b)就发生了缩颈，因而短路后很快完成过渡，电流无明显上升，且亚射流过渡的短路均发生在脉冲电流期间．图 4c，d 是对应于图 3c 的两组短路过渡的高速摄像，从摄像可以

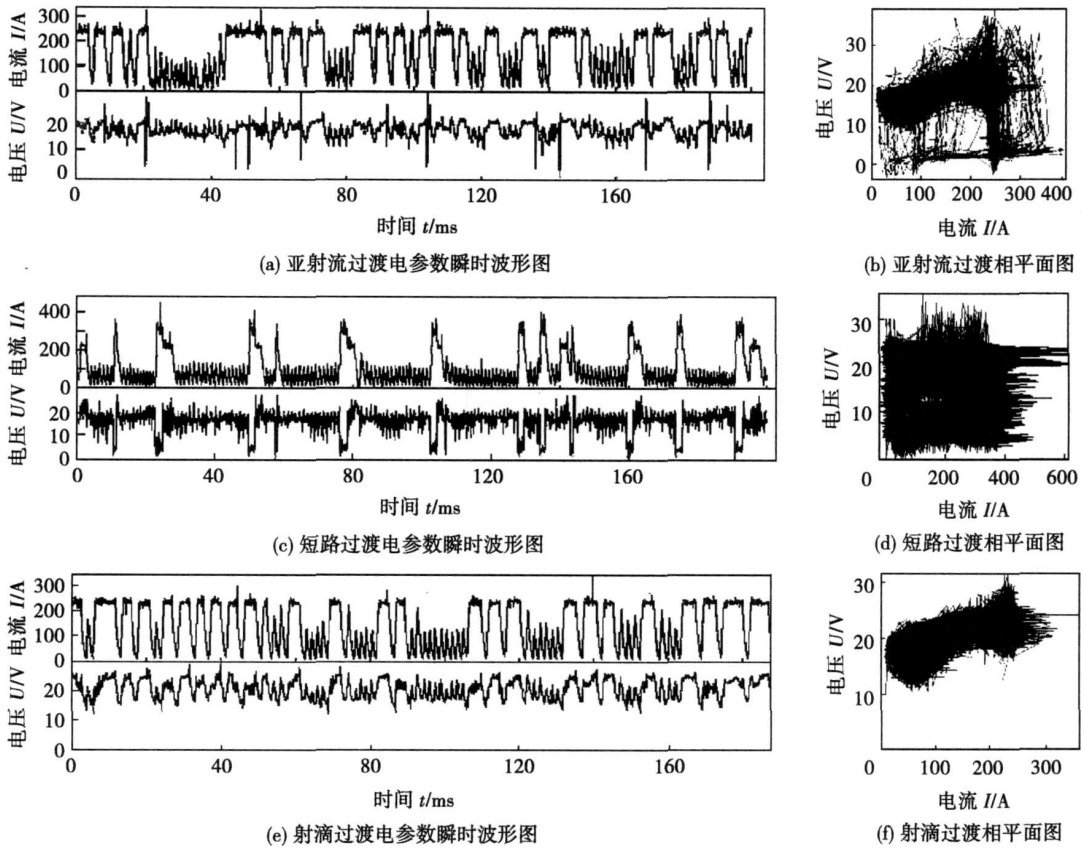

图 3　铝脉冲 MIG 焊自适应控制试验波形

Fig. 3　Control waves of self-adapting control in pulse MIG welding

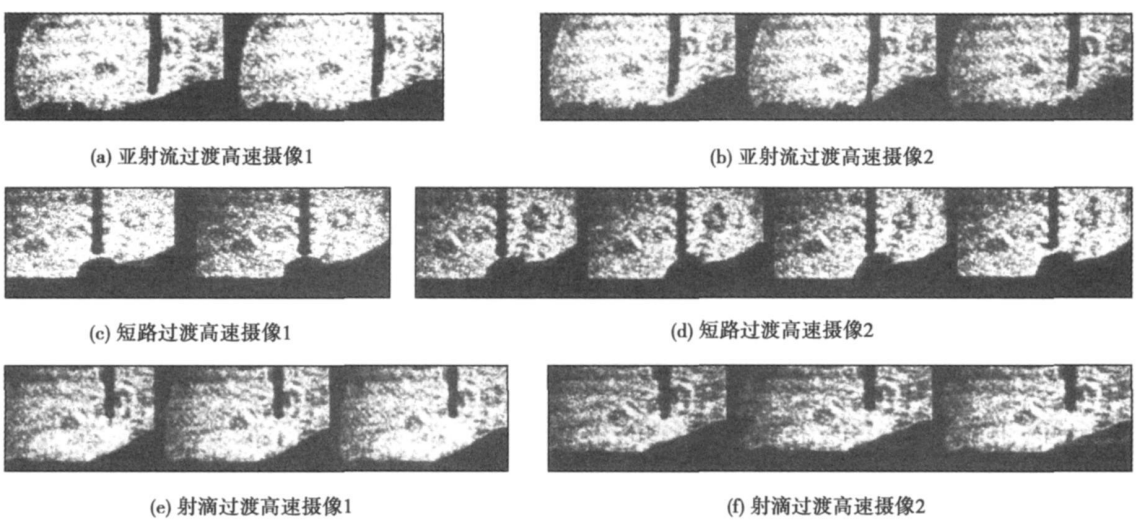

图 4　脉冲 MIG 焊自适应控制过程的同步高速摄像(1 000 幅/ s, φ1. 6)

Fig. 4　High speed camera images of self-adapting control in pulse MIG welding

看出，熔滴短路前未产生缩颈，短路时间较长，短路时电流快速上升，短路后甚至会甩出部分熔滴(图 4d)，造成飞溅. 图 4e，f 是对应于图 3e 的 33 ~ 35 ms 和 71 ~ 73 ms 的两组射滴过渡的高速摄像，前者射滴过渡发生于脉冲电流的上升时，后者发生于脉冲电流的下降时，并无特别规律，这与一般一脉一滴过渡控制熔滴过渡多产生在脉冲电流后期是不同的；所过渡的熔滴沿轴向过渡，直径也小于焊丝直径.

3 讨论与分析

在短路过渡和亚射流过渡中，都存在短路过程，有关的电弧理论研究表明[4]：对短路过渡的电弧中焊丝端部熔滴影响较大的主要有电磁收缩力和表面张力．悬垂在焊丝端部的熔滴非常接近于自由液柱的条件，其几何形状与承受周期性变形的液柱几何形状间关系的模型[4]，如图 5，焊丝端部熔滴的模型的纵切面取正弦波，这样的外形对焊丝端部的熔滴是现实的．由于焊丝直径的约束，将熔滴变换为等效液柱的初始半径为 $R=(R_e+R_d)/2$.

由此模型得到的液柱失稳的临界波长为

$$\lambda_c=\frac{2\pi R}{(1+\frac{\mu_0 I^2}{2\pi^2 R\sigma})^{\frac{1}{2}}}$$

设产生自由过渡的熔滴体积为 $4\pi R_d^3/3$[4]，且 $R_d=1.2R_e$；对于直径($2R_e$)为 1.6 mm 的铝合金焊丝，$R=0.88$ mm，$2R_d=1.92$ mm；对于铝合金，取表面张力 $\sigma=0.5$ N/m，利用上式做一估算．

当电流 $I=50$ A 时，$\lambda_c=4.85$ mm$>2R_d$，不失稳；当电流 $I=235$ A 时，$\lambda_c=1.84$ mm$<2R_d$，失稳．而同等条件下，钢的 λ_c(表面张力取 1.2 N/m) 分别为 5.15，2.66 mm.

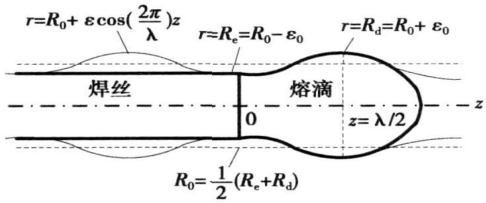

图 5 焊丝端部受正弦扰动的熔滴几何形状模型

Fig. 5 Shape model of melt drop at tip of welding wire with sine perturbation

虽然是估算，但也在相当程度上说明了表面张力在铝 MIG 焊短路过程中的重要作用．由于电磁收缩力与材料无关，主要取决于电流的大小，在相同的电流下，表面张力小的熔滴更容易失稳；铝熔滴的表面张力较小，在焊丝端部不易形成较大直径的熔滴，很容易失稳形成过渡．

从图 4a，b 可以看出，在较大电流下，熔滴易失稳形成缩颈；在电弧较短时，可形成短路，因已形成缩颈，电流上升不大即可缩断，短路时间很短，这样产生亚射流过渡．

从图 4c，d 可以看出，在较小电流下，熔滴不易失稳缩颈，在焊丝端部形成较大熔滴，最终形成短路；因没有提前形成缩颈，电流迅速上升，在短路的条件下缩颈而缩断，短路时间较长，这样产生短路过渡；在熔滴缩断的瞬间，电流很大且仍处于上升期，所产生的电磁收缩力无论是大小还是其变化率，都会给焊丝端部残留的熔滴很大的向上的力以及对正向熔池中铺展的熔滴很大的向下的力，这很容易产生飞溅．

从图 4e，f 可以看出，在较大弧长条件下，熔滴易失稳形成过渡，不易形成短路．可能在电流较小的条件下在焊丝端部积累较大熔滴，当电流上升时，熔滴临界尺寸减小而失稳形成缩颈，进而缩断，熔滴沿轴向过渡(图 4e)；也可能在电流较大的条件下在焊丝端部产生较大熔滴，超过熔滴临界尺寸而失稳缩颈并缩断，熔滴沿轴向过渡，这样产生射滴过渡．

电弧中还存在多种机械作用力，其中等离子流力是电弧的主要机械作用力[4]，上述分析并未考虑等离子流力，尤其在弧长较大的射滴过渡时，等离子流力仍会有较大作用，因而实际的熔滴临界尺寸会更小．

4 结 论

(1) 在铝脉冲 MIG 焊亚射流过渡自适应控制的条件下，亚射流过渡的熔滴在短路瞬间或即将发生短路时，就已经产生了缩颈，因而短路后就迅速缩断，短路时间很短，短路电流上升不明显．铝这种熔滴过渡的特点与其表面张力小应有密切关系，在大电流下焊丝端部不易保持较大熔滴，亚射流过渡的范围受到限制．

(2) 选择合适的自适应控制参数可以将铝脉冲 MIG 焊控制在亚射流过渡的范围内；若控制参数不合适，会出现射流过渡、短路过渡等过程．通过对焊接电流、电压的时基瞬时波形和相平面图以及高速摄像的研究，证明了较为精确的控制参数对亚射流过程的重要影响．

参考文献：

[1] 胡特生. 电弧焊[M]，北京，机械工业出版社，1996.

[2] Halmoy E. Electrode melting in arc welding[M]. Gasgow(VK): Physical Aspects of Arc Welding, 1993.

[3] 杨立军，张 健，李志勇，等. 铝脉冲 MIG 焊亚射流过渡的自适应控制[J]. 焊接学报，2007，28(4)：93－96.
Yang Lijun, Zhang Jian, Li Zhiyong, *et al*. A self-adapting control method of Al pulsed-MIG welding for meso-spray transfer[J]. Transactions of the China Welding Institute, 2007, 28(4): 93－96.

[4] Lancaster J F. The physics of welding[M]. Oxford, Pergamon Press, 1984.

作者简介：杨立军，男，1966 年出生，博士，副教授．主要从事焊接电源及设备的控制以及焊接物理方面的工作．已发表学术论文 30 余篇．

Email：yljabc@tju.edu.cn

MAIN TOPICS, ABSTRACTS & KEY WORDS

Effect of H_2 flow rate on electrical conductivity of APS TiO_2 coatings HE Dingyong, ZHANG Hua, JIANG Jianmin, LI Xiaoyan (Beijing University of Technology, Beijing 100124, China). p 1—4

Abstract: TiO_2 coatings were produced by atmospheric plasma spraying system. H_2 flow rate was adjusted to investigate its effect on the microstructure, phase and electrical conductivity of TiO_2 coatings. The results show that TiO_2 coating is mainly composed of rutile, anatase and deoxidization phases Magneli (Ti_nO_{2n-1}, n = 4—10), and the contents of them depend on H_2 flow rate. With the increasing of H_2 flow rate, porosity decreases, deoxidization phase Magneli and the electrical conductivity of coatings increase. The electrical conductivity of TiO_2 coatings also increases with temperature.

Key words: TiO_2 coating; atmospheric plasma spraying; H_2 flow rate; electrical conductivity

Numerical simulation of effects of scanning path on electron beam selective melting process of Ti-6Al-4V QI Haibo[1,2], YANG Minghui[1], QI Fangjuan[1] (1. School of Material Science and Engineering, Shijiazhuang Railway Institute, Shijiazhuang 050043, China; 2. Department of Mechanical Engineering, Tsinghua University, Beijing 100084, China). p 5—8

Abstract: Aimed at the influence of temperature distribution on forming parts caused by scanning paths of filling line of electron beam selective melting technology, finite element mode with actual conditions was established and elements belonging to the rotated part were arranged in accordance with the loading sequence. Simulation results show that comparing with long-side scanning, short-side scanning and sub-area scanning, the rotated scanning of rectangular part can greatly decrease temperature gradient in the begin point and the end point of the first scanning line, especially there is a positive temperature gradient in the end point which can avoid the temperature decreasing of the molten metal. Combining rotated scanning with reversing scanning, the uniformity degree of temperature in rectangular part has greatly improved and the curl distortion caused by thermal stress has also decreased. The horizontal tensile strength of the Ti-6Al-4V tensile specimens prepared by the above optimized scanning method is 1 080 MPa.

Key words: electron beam selective melting; scanning path; numerical simulation; rotated scanning; reversed scanning

Control and process of high speed short circuit arc welding HUANG Pengfei[1], LU Zhenyang[1], SUN Zhigang[2], WEI Jian[2], YIN Shuyan[1] (1. College of Mechanical Engineering and Applied Electronics Technology, Beijing University of Technology, Beijing 100124, China; 2. Nantong CIMC Tank Equipment Co, Ltd, Nantong 154007, China). p 9—12

Abstract: Short circuit arc welding parameters and waveform control are researched on the basis of IGBT inverter welding power supply. Under the same welding current, optimum arc voltage will decrease with the increasing of welding speed. And it is proved that hard arc is more stable under lower voltage, which is suitable for high speed welding. The relationships among energy input, arc voltage dropping speed and arc stability are studied, and it is demonstrated that a lower voltage dropping speed will lead to a higher arc energy, but the adjust time of voltage should be less than average arc time. The welding experiments prove that the weld appearance and fusion are good when the welding speed is 1.5 m/min, which meet the requirements of container manufacturing.

Key words: high speed welding; short circuit; parameter; arc energy

Microstructure and wear resistance of argon arc cladding Ni-Mo-Zr-WC-B_4C composite coating WANG Zhenting, QIN Lifu (College of Materials Science and Engineering, Heilongjiang Institute of Science and Technology, Harbin 150027, China). p 13—16

Abstract: α-Fe-based composite coating reinforced by (Fe, Mo, W, Zr)$C_{0.7}$, (Fe, Mo, W, Ni)$_2$B, (Fe, Mo, W, Ni, Zr)(B, C) particles were prepared on the surface of Q235 steel by means of argon arc cladding technique with the pre-alloyed powder of Ni, Mo, Zr, WC and B_4C. The microstructure and properties of the coating were investigated by scanning electron microscope, X-ray diffractometer, microhardness tester and friction and wear machine. The results indicate that the coating has excellent bonding between the coating and the Q235 steel substrate and is uniform, continuous and almost defect free. The particles are evenly distributed in the clad coating; composite coating has high hardness, which the average hardness of the coating is about HV1300. The argon arc clad composite coating has high hardness and excellent wear resistance under dry sliding wear test conditions, and the wear resistance of the coating is 14 times more than that of the matrix.

Key words: argon arc cladding; in-situ synthesis; composite; wear resistance

Metal transfer under self-adapting control of meso-spray in pulse MIG welding of aluminum YANG Lijun[1], LI Zhiyong[2], LI Huan[1], LI Junyue[1] (1. Tianjin Key Laboratory of Advanced Joining Technology, Tianjin University, Tianjin 300072, China; 2. School of Material Science and Engineering, North University of Chi-

na, Taiyuan 030051, China). p 17—20

Abstract: The metal transfer behavior of meso-spray transfer is studied under self-adapting control of meso-spray in pulse MIG welding of aluminum. The main acting forces against a droplet and the important role of surface tension are analyzed by the waves testing and high speed camera of short circuit, meso-spray and spray from different parameters in pulse MIG welding. The results of experiment demonstrate that a self-adapting process should be accurately controlled for the narrow working range of meso-spray transfer in pulse MIG welding of aluminum, and the proposed control parameters can make the arc running within the narrow range and the special droplet transfer process stable.

Key words: aluminum; pulse MIG welding; self-adapting control; droplet transfer; high speed camera

Pre-processing software for three-dimensional simulation and prediction of weld solidification cracks DONG Zhibo[1], ZHAN Xiaohong[2], WEI Yanhong[1,2], LU Yafeng[3], GUO Ping[3], YANG Yongfu[3] (1. State Key Laboratory of Advanced Welding Technology Production, Harbin Institute of Technology, Harbin 150001, China; 2. Department of Material Science and Technology, Nanjing University of Aeronautics and Astronautics, Nanjing 210016, China; 3. Titanium Alloy Institute, Northwest Institute For Non-ferrous Metal Research, Xi'an 710016, China). p 21—24

Abstract: A software consisted of pre-processing, post-processing and solidification cracks predicting subsystems is developed, which can simulate and predict the weld solidification cracks with three dimensional FEM. The pre-processing helps users to choose the workpiece, to input the thermal-mechanical properties of materials and welding parameters, to set boundary conditions, and to automatically generate command streams of MSC. Marc to create process files for final FEM calculation. Furthermore, system can transfer the process files to software package of MSC. Marc to complete the calculation of thermal, strain and stress distributions in background. Therefore, the simulated results are prepared for the post-processing.

Key words: solidification cracking; pre-processing; simulation and prediction

Full digitalized welding power platform with multi-function purposes SHA Deshang[1], LIAO Xiaozhong[1], SHAN Lijun[2], BAO Yunjie[2] (1. School of Automation, Beijing Institute of Technology, Beijing 100081, China; 2. Beijing Time Technology Company Ltd, Beijing 100085, China). p 25—28

Abstract: A welding platform used in shielded metal arc welding, TIG, CO_2 short-circuit GMAW, single pulsed MIG/MAG and double pulsed MIG/MAG welding is established. The platform is composed of welding power, wire feeder and water cooler, which operation principles and main function are analyzed. The full digital control theories of short circuiting transfer, single pulsed and double pulsed MIG/MAG are explained in detail. Experimental results of a 400 A prototype show that it is feasible to apply different welding methods only by changing software and without changing any hardware, and the welding performance is also perfect.

Key words: welding power; full digital control; gas metal arc welding

Influence of nano-Al_2O_3 suspension concentration on forming of plasma spraying coating FAN Xiangfang, QIU Changjun, CHEN Yong (College of Mechanical Engineering, Nanhua University, Hengyang 421001, China). p 29—32

Abstract: The nano-alumina coating was prepared by suspension plasma spraying under atmospheric conditions, and the effect of nano-Al_2O_3 suspension concentration on forming of plasma spraying coating was studied by scanning electron microscopy and theory analyses. The results show that the concentration of nano-Al_2O_3 suspension has a significant influence on the size of droplet, the enthalpy needed for spraying suspension, the roughness of coatings surface and the microstructure of coatings. Low concentration of the suspension is beneficial for fine nanostructures coatings, which means low spraying efficiency. The optimized concentration of nano-alumina suspension is between 5%(wt) and 10%(wt).

Key words: nano-alumina; suspension concentration; plasma spraying; coating forming

Effect of alloying elements on intermediate temperature filler metal in stepped welding of 6063 aluminum alloy ZHU hong[1,2], XUE Songbai[1], SHENG Zhong[1] (1. College of Materials Science and Technology, Nanjing University of Aeronautics and Astronautics, Nanjing 210016, China; 2. The 14th Research Institute, China Electronic Technology Group Corporation, Nanjing 210013, China). p 33—36

Abstract: The contents of Si, Cu, Ni and RE are changed by using orthogonal test in order to study the effect of the content changes on the melting points, spreading property and shear strength of Al-Si-Cu-Ni-RE, and the microstructure of filler metal is analyzed by SEM and EDS. It is indicated that the spreading area is mainly affected by the composition of filler metal and temperature; the DSC results show that Cu has the most important influence on the melting points filler metal, which decreases sharply with the Cu content increasing, and then Ni, Si and RE come second; the black brittle phase θ ($CuAl_2$) and the macrosegregation flocculent phase go against the performance of joint, but the matrix phase α (Al) with face-centered cubic solid solution and the Si phase with conglobulation make the performance of joint better.

Key words: orthogonal test; spreading property; melting point; microstructure

Effect of zinc coating on arc heating behavior for joining Al and zinc coated steel by welding-brazing process ZHANG Hongtao[1], FENG Jicai[2], HE Peng[2], ZHAO Hongyun[1] (1. School of Materials Science and Engineering, Harbin Institute of Technology at Weihai, Weihai 264209, China; 2. School of Materials Science and